ADVANCED HEALTHCARE MATERIALS
www.advhealthmat.de

Advances in Nanoporous Anodic Alumina-Based Biosensors to Detect Biomarkers of Clinical Significance: A Review

Gayathri Rajeev, Beatriz Prieto Simon, Lluis F. Marsal, and Nicolas H. Voelcker**

There is a strong and growing demand for compact, portable, rapid, and low-cost devices to detect biomarkers of interest in clinical and point-of-care diagnostics. Such devices aid in early diagnosis of diseases without the need to rely on expensive and time-consuming large instruments in dedicated laboratories. Over the last decade, numerous biosensors have been developed for detection of a wide range of clinical biomarkers including proteins, nucleic acids, growth factors, and bacterial enzymes. Various transduction techniques have been reported based on biosensor technology that deliver substantial advances in analytical performance, including sensitivity, reproducibility, selectivity, and speed for monitoring a wide range of human health conditions. Nanoporous anodic alumina (NAA) has been used extensively for biosensing applications due to its inherent optical and electrochemical properties, ease of fabrication, large surface area, tunable properties, and high stability in aqueous environment. This review focuses on NAA-based biosensing systems for detection of clinically significant biomarkers using various detection techniques with the main focus being on electrochemical and optical transduction methods. The review covers an overview of the importance of biosensors for biomarkers detection, general (surface and structural) properties and fabrication of NAA, and NAA-based biomarker sensing systems.

1. Introduction

A compound the presence of which in body fluids like blood, saliva, and urine, or the variation in concentration of which indicates a physiological disorder, state, or risk factors in an organism, is termed a biomarker. The presence, absence, or variation in concentration of a biomarker usually indicates whether there is a risk of a disease, if a disease already exists or how the disease may develop.[1] Biomarkers have been used for a long time by scientists, epidemiologists, and physicians for studying human diseases. The practice of using biomarkers in both preclinical studies and clinical diagnostics started a long time ago.

Currently, most biomarker analyses for diagnosis and prognosis of various diseases are conducted in dedicated laboratories using large equipment and trained personnel. Biomarker analyses are not only expensive but also time consuming and often involve a waiting period in order to obtain results. Therefore, there is a growing demand for highly efficient analytical devices in clinical diagnostics that deliver sensitive, cheap, and rapid detection and quantification of biomarkers. The development of novel biosensing systems based on state-of-the-art nanotechnology and nanoscience is being hailed as breakthrough and may well meet the above demand. According to the definition of the International Union of Pure and Applied Chemistry (IUPAC), a biosensor is "a device that uses specific biochemical reactions mediated by isolated enzymes, immunosystems, tissues, organelles, or whole cells to detect chemical compounds usually by electrical, thermal, or optical signals."[2] Immense research efforts are being conducted dedicated to the development and application of biosensing systems for detection of biomarkers of clinical significance like nucleic acids, antigens, pathogens, and enzymes. At the same time, it is also important to bring this technology to potential end users by translating biosensors into everyday devices, in particular at the point-of-care (POC). Advances in nanotechnology offer new technologies for POC diagnostics and user-friendly analytical devices, permitting miniaturization and avoiding the need of specialized equipment or expert technicians.

Nanomaterials have recently been used by researchers to develop ultrasensitive biosensors for biomarker detection owing to their unique physical and chemical properties. The large surface area of nanomaterials allows the immobilization of an increased quantity of bioreceptor units. This often leads to an enhanced sensing performance with increased sensitivities

Dr. G. Rajeev, Dr. B. Prieto Simon, Prof. N. H. Voelcker
Future Industries Institute
Mawson Lakes, SA 5095, Australia
E-mail: beatriz.prieto-simon@monash.edu;
nicolas.voelcker@monash.edu
Dr. B. Prieto Simon, Prof. N. H. Voelcker
Monash Institute of Pharmaceutical Sciences
Monash University
Parkville, VIC 3052, Australia
Prof. L. F. Marsal
Departamento de Ingeniería Electrónica
Eléctrica y Automática
Universitat Rovira i Virgili
Avda. Països Catalans 26, 43007 Tarragona, Spain
The ORCID identification number(s) for the author(s) of this article can be found under https://doi.org/10.1002/adhm.201700904.

DOI: 10.1002/adhm.201700904

and lowered limits of detection. Also, certain nanomaterials possess innate properties (e.g., optical and electronic properties) which themselves are exploited to develop effective transduction methods. Holzinger et al.[3] recently reviewed the use of various nanomaterials in biosensing. Among these, polymeric, magnetic, and metal nanoparticles, quantum dots, carbon nanotubes, graphene, and porous materials (e.g., porous silicon, porous gold, porous alumina, porous carbon) are popular choices. Advancements made in this area have enabled the development of various highly efficient biosensing systems which fulfill the demand for cost-effective and rapid devices.

Nowadays, there is an increasing interest in using nanoporous materials for developing biosensors.[4] This interest is a result of those materials having interesting properties like enhanced surface-to-volume ratio, thermal, chemical, and mechanical stability (this is particularly relevant for retaining activity of enzymes in enzymatic sensors), and tunable pore geometry which can contribute to enhance the analytical performance of biosensors. Over the past decade, the use of single or arrays of nanochannels for biosensing applications has been burgeoning. Nanochannel-based devices have been inspired by protein-based ion channels in living systems used for electrical signaling in nerves and muscles.[5]

Among nanoporous materials, those prepared by self-ordering electrochemical anodization are of particular interest. Advantages of this fabrication process over other methods such as lithographic techniques are that the fabrication itself is simple, highly parallel, and cost effective. Moreover, this process generates nanochannel arrays which are highly ordered and vertically aligned. The most significant example of such kind of nanoporous material is nanoporous anodic alumina (NAA), which not only has unique chemical, mechanical,[6] optical, and electrical properties but also has high thermal stability,[7] biocompatibility, and high surface-to-volume ratio.[8] Chemical properties of NAA, particularly the large amount of hydroxyl groups present on the nanochannels, allow facile biofunctionalization for an efficient and simple immobilization of bioreceptors. Due to these properties, this material has the potential to develop biosensing devices with excellent analytical performance.

Due to the high demand for high-performance biosensors for analysis of biomarkers in clinical diagnostics and the potential of NAA for development of smart sensing devices, we review here the advances in the use of NAA as a sensing platform for detection of clinically significant biomarkers. We begin by discussing the significance of various biomarkers of particular interest in clinical diagnosis, and the challenges to develop bioanalytical systems for them. Then we discuss the fabrication methods, unique structural, chemical, optical, and electrical properties of NAA that make this material a suitable sensing platform for biomarkers. After this, we focus on various examples of the use of NAA to develop biosensors for the electrochemical and optical detection of biomarkers such as pathogens, nucleic acids, proteins, antigens, enzymes, and hormones, either exploiting NAA directly as sensing platform or as a template of ordered nanostructured transducers. We conclude the review by discussing the demand for biosensing platforms for detection of biomarkers that have not

Gayathri Rajeev is a Ph.D. student at Future Industries Institute, University of South Australia (UniSA). She finished her B.Tech. and M.Tech. in Nanotechnology at Amity University (2013) in India. She did her masters research at Mawson Institute (UniSA) in 2014 and obtained the University President's Scholarship to pursue her Ph.D. at UniSA. Her research focuses on fabrication of nanoporous anodic alumina structures and their application in electrochemical and optical biosensing for monitoring the healing trajectory of chronic wounds. She is the student representative and also an active member in the management committee of the Australian Nanotechnology Network (ANN) since 2015.

Beatriz Prieto-Simón received her Ph.D. in chemistry from the Universitat Autònoma de Barcelona in 2005. At present, she is a research fellow at the University of South Australia leading a research line on nanostructured electrochemical biosensors. She has made significant contribution to the fields of biosensors, biomaterials, nano- and biotechnology, and the crossing over into areas such as environmental control and food safety. Currently, her research is focused on combining the advantages of novel nanostructured materials, site-specific immobilization of bioreceptors, and new electrochemical techniques, to provide platforms for sensitive and selective multiplexed detection.

Nicolas Voelcker completed his Ph.D. thesis in 1999 in polymer surface chemistry at the DWI Leibniz Institute for Interactive Materials. He is the Scientific Director of the Melbourne Centre for Nanofabrication, professor at the Monash Institute of Pharmaceutical Sciences at Monash University, and science leader at the Commonwealth Scientific and Industrial Research Organisation (CSIRO). His key research interest lies in the fabrication and surface modification of porous semiconductor materials for applications in biosensors, biochips, biomaterials, and drug delivery. A core research activity in his laboratory is the study of porous silicon based nanostructures and their surface chemistry.

received significant attention (e.g., exosomes) and prospective advances in this research field to benefit the human kind.

2. Background: Significance of Biomarkers in Clinical Diagnostics

Biomarkers are defined by the National Institutes of Health as compounds that are objectively measured and evaluated as an indicator of normal biological processes, pathogenic processes, or pharmacological responses to a therapeutic intervention.[9] Biomarkers are found in body fluids such as blood, serum, urine, wound fluid, and saliva.

2.1. State of the Art and Limitations in Existing Analytical Systems for Biomarkers Detection

The practice of detecting biomarkers for diagnosis or monitoring the status of a disease ages back to the beginning of medical practice.[1] In 350 BC, Hippocrates adapted physical inspection (such as body temperature, heart rate, and general physical features) and visual analysis of body fluids to diagnose bodily conditions, particularly uroscopy, visually examining urine of patients to look for chronic illnesses.[10] Advances in clinical diagnosis evolved through the following centuries with the invention of stethoscope, ophthalmoscope, laryngoscope, spirometer, electrocardiogram, microbiological techniques, X-ray, radiology, and so on. The importance of biomarkers for diagnosis of major diseases such as cancer and heart disease has been discussed since at least the 1980s.[11] The number of clinical laboratories is growing, and so is the quest for advanced technologies for clinical analytical methods. Currently, most diagnostics rely on chemical analysis of body fluids in a clinical setting using advanced techniques such as chromatographic separation coupled to mass spectrometry, immunohistochemistry, enzyme-linked immunosorbent assay (ELISA), polymerase chain reaction (PCR), flow cytometry, or microscopy. These techniques are often expensive, time-consuming, and require a trained technician to perform the tests. The ideal diagnostic techniques are those that allow the test to be done in a decentralized setting (general practitioner's office, home, ambulance, offices), rapid, highly sensitive, and require low volumes of sample. We are still at the infancy of POC diagnostics such as paper-based[12] and smart phone-based[13] POC diagnostics in a practical point of way. But in the future, we envision POC diagnostics becoming common place the major concerns of their development, such as sample pre-treatment, handling complex body fluids with minimal matrix effects, are addressed.

2.2. Potential Biomarkers of Interest in Clinical Diagnostics

Biomarker analysis has a wide range of applications which begins from the most obvious disease diagnosis as discussed earlier, as well as several other uses such as drug development, development of personalized medicine, drug validation, and prognosis of an existing condition.[1] However, we limit our scope in discussing the importance of biomarkers for disease diagnosis and prognosis.

The most popular biomarkers of interest at present include but are not limited to those related to cardiovascular diseases, cancer, sepsis, asthma, neurological disorders, inflammatory disorders, and infectious diseases. In this review, we introduce a classification of biomarkers based on their biological nature/function which is given in **Table 1**. Diseases caused by pathogens, commonly termed as infectious diseases such as tuberculosis, acquired immuno deficiency syndrome (AIDS) and malaria account for almost 25% of deaths across the world of which nearly 95% seem to be in developing countries owing to the inability to afford expensive diagnostics.[14] One million infants die every year in Africa due to malaria although the disease is curable. This is due to the unavailability of an affordable POC device for the accurate and early diagnosis of the parasites causing malaria to allow immediate treatment. Human immuno deficiency virus (HIV) for AIDS, Dengue virus (DENV) for Dengue fever, and *Escherichia coli* (*E. coli*) bacterium for anemia/kidney failure/diarrhea, are other important pathogen biomarkers related to infectious diseases.

Another major cause of mortality and morbidity across various countries is cancer. Early diagnosis is the only way to increase the probability of patient survival. Most important biomarkers associated with cancer are proteins/antigens (e.g., prostate-specific antigen (PSA), α-fetoprotein, carcinoembryonic antigen, cancer antigens 125, 19-9, and 15-3 (CA 125, CA 19-9, and CA 15-3)), whole cells (e.g., circulating tumor cells), cytokines (e.g., interleukin-6 (IL-6) and interleukin-8 (IL-8)), and hormones (e.g., β-human chorionic gonadotropin (β-hCG)).[15] Exosomes are another powerful class of biomarkers which is gaining interest rapidly, and are considered the future of biomarkers in medicine.[16] Exosomes are lipid-encapsulated nanoscale vesicles which are released by certain cells into the extracellular fluid for intercellular signaling, regulation of cellular pathways in recipient cells, and waste management. Exosomes harbor proteins on their outer surface which serve as biomarkers that otherwise have a low expression and cannot be normally detected. Endogenous biomolecules of exosomes, such as microRNA, can be used as biomarkers for early diagnosis of conditions like cancer and neurodegenerative diseases. However, related research is still in its infancy and there is an exponentially growing interest for a deeper understanding of exosome-related biology. Major challenges include effective biomarker release from exosomes, avoiding degradation, and the complexity of endogenous molecules which can cause interference.[17]

Cardiovascular diseases (CVD) are another leading cause of death worldwide, with myocardial infarction and stroke being the most common ones. Biomarkers related to them include lipids (LDL-cholesterol, triglycerides), regulatory proteins/peptides (B-type natriuretic peptides, cardiac troponins I, C, and T (cTnI, cTnC, cTnT)), and cardiac enzymes (creatine kinase, lactate dehydrogenase, aspartate transaminase). Certain inflammatory biomarkers are also used for predicting the risk of certain CVD, such as cytokines (e.g., tumor necrosis factor-α (TNF- α)), enzymes (e.g., matrix metalloproteinases (MMPs)), growth factors (e.g., vascular endothelial growth factor (VEGF), epidermal growth factor (EGF), and fibroblast growth factor (FGF)).[18]

Table 1. Classification of biomarkers of interest and biosensors developed for their detection using NAA.

Biomarker category	Key examples	Associated disease	Sensing technique	LOD	Reference
Pathogens	WNV-DII	West Nile Fever	DPV	4 pg mL^{-1}	[49]
	E. coli	Foodborne diseases	EIS	10 CFU mL^{-1}	[50a]
			DPV	22 CFU mL^{-1}	[50b]
			EIS	84 CFU mL^{-1}	[56]
	DENV2	Dengue fever	DPV	1 PFU mL^{-1}	[51a]
				1 PFU mL^{-1}	[51c]
			EIS	0.2 PFU mL^{-1}	[51d]
	Legionella pneumophila	Legionnaires' disease	DPV	3.1×10^{-13} M	[52]
	S. aureus	UTI, kidney failure, anemia	EIS	100 CFU mL^{-1}	[50c]
Small molecules	Glucose	Hyper/hypoglucemia	Amperometry	0.01 M	[59a]
			Amperometry	1×10^{-6} M	[59c]
			Voltammetry	0.1×10^{-6} M	[59b]
			Photoluminescence	0.1 M	[39]
	Cholesterol	Hypertension, CVD	Amperometry	1.8×10^{-4} M	[60a]
			Amperometry	0.5 mg mL^{-1}	[60b]
	Dopamine	Neurological disorders	Amperometric-using ISFET	2 µmol L^{-1}	[64]
	Urea	Liver diagnosis	Piezoelectric-enzymatic	0.05×10^{-6} M	[61b]
Proteins	CRP	CVD	LSPR, IRS	1 fg mL^{-1}	[43c]
			LSPR, IRS	1 pg mL^{-1}	[33]
	CA 15-3	Breast cancer	Voltammetry	52 U mL^{-1}	[69a]
	Human IgG	Model system	Voltammetry	98 µg mL^{-1}	[32]
			Interferometry	0.1 mg mL^{-1}	[41a]
	Botulinum neurotoxin A	Botulism	EIS	500 pM	[71]
	PTHrP	Cancer biomarker	Voltammetry	50 ng mL^{-1}	[70]
	Avidin	Model system	LSPR	10 µg mL^{-1}	[43b]
	Biotin	Model system	EIS	–	[63a]
	Glucose oxidase	Model system	Voltammetry	100 ng mL^{-1}	[54]
	Trypsin	Pancreatitis	PL	0.1 mg mL^{-1}	[40a]
			PL	40 µg mL^{-1}	[40b]
Nucleic acid	DNA		Voltammetry		
			Voltammetry		
			EIS	0.1×10^{-9} M	[76]
			EIS, CV	42 ng mL^{-1}	[75]
			EIS	12.5×10^{-9} M	[79]
			IRS	–	[74]
			EIS	50×10^{-12} M	[78]
			FRET	2×10^{-9} M cm^{-12}	[80]
				3.1×20^{-13} M	[52]
				–	[81]

Chronic wounds including diabetic foot ulcers, venous leg ulcers, and pressure ulcers are a major concern in an ageing population. Potential biomarkers of interest for chronic wound management include biofilms, cytokines, nucleic acids, enzymes like MMPs and extracellular matrix (ECM), exposed bone, growth factors and hormones, nutritional factors like zinc, glutamine, and vitamins, reactive oxygen species (ROS), pH of wound fluid, temperature, and transepidermal water loss from periwound skin.[19]

As shown above, for any physiological disorder, biomarkers can take various forms such as proteins and peptides (PSA indicates risk of prostate cancer, MMPs for nonhealing wounds), small molecules (cholesterol for CVD, glucose for diabetes mellitus), nucleic acids (circulating nucleic acids in breast cancer), pathogens (HIV for AIDS), and whole cells (white blood cells for cancer or infections).

In this review, we limit ourselves to discuss biosensing systems for the detection of biomarkers of clinical significance developed using NAA as a sensing platform.

3. NAA: Fabrication, Functionalization, and Properties

In the last decade, NAA has emerged as a versatile platform for a multitude of sophisticated applications such as in biosensing, molecular separation, cell adhesion, catalysis, drug delivery, template synthesis, solar cells, energy storage, cell growth, and data storage. NAA is characterized by its homogenous and self-ordered nanopores. It is formed by anodization of high-purity Al in acidic solution by applying a specific voltage which causes self-ordering pore formation and results in a highly ordered 3D porous structure.[20] NAA has a honeycomb structure which consists of a closely packed hexagonal array of cells with cylindrical nanopores in the center of the cells that runs perpendicular to the surface of the underlying Al substrate. The geometrical structure of NAA is characterized by its pore diameter (d_p), interpore distance (d_i), pore length (l_p), barrier layer thickness, and wall thickness (**Figure 1**). These parameters can be finely tuned by controlling the anodization conditions such as type of electrolyte, electrolyte composition, temperature, anodization voltage, current, and time. By tuning these parameters, a range of geometric features can be obtained like 10–400 nm for pore diameter, 50–900 nm for interpore distance,[21] 10 nm to several hundreds of μm for pore length, and porosity from 5 to 50%.[22] Pore density can be tuned in a range from 10^9 to 10^{11} pores cm^{-2}.[23]

Self-ordering of pores and formation of long-range pore order require pre-treatment of the Al surface to obtain a smooth surface. The most commonly used method for Al pre-treatment is electropolishing in a mixture of perchloric acid and ethanol in 1:4 ratio at 20 V for 5 min at 5 °C. While the method using perchloric acid is very effective, it also involves various drawbacks since hot perchloric acid has a high hazardous nature. The use of perchloric acid requires special handling such as dedicated fumehood, continuous cooling systems, and wash-down systems in the fumehood to prevent the formation of perchlorate crystals on the fumehood walls. Perchlorate crystals are shock-sensitive and highly explosive in nature. To address this issue, an alternative method for Al pre-treatment has been reported, which is called "chemical polishing." In this method, Al is boiled in a mixture of nitric and phosphoric acids and the resulting smoothness of the surface is comparable to that produced by electropolishing.[24]

Long-range ordering of NAA occurs under specific anodizing conditions. Most commonly used electrolytes for the conventional anodization process known as mild anodization are sulfuric, oxalic, and phosphoric acids.[25] Long-range ordering occurs within the three well-known growth regimes which are 25, 40, and 195 V using sulfuric, oxalic, and phosphoric acid, respectively.[22,26] Under these specific conditions, pore formation occurs by two overlapping processes in equilibrium which are the formation of aluminum oxide (alumina) at the oxide/Al interface and the electric field-assisted dissolution of alumina at the pore bottom oxide/electrolyte interface by keeping the pore walls intact. The resulting NAA structure has an oxide barrier layer at the pore bottom, which has to be removed for many applications (pore opening).[27,28] This has been achieved by chemical etching in 5% aqueous solution of phosphoric acid, ion beam, or plasma etching. This chemical method is used to

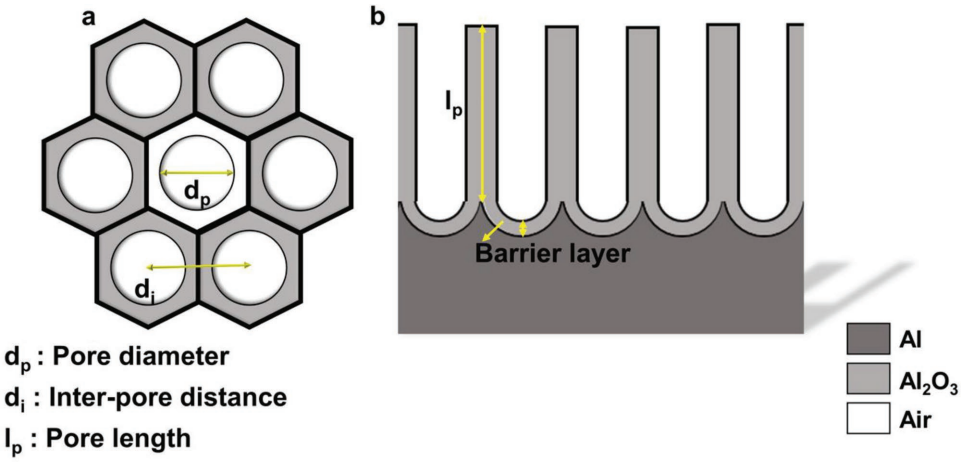

Figure 1. Schematic of the geometrical structure of NAA showing a) top and b) cross-sectional views.

enlarge the pore diameter keeping interpore distance constant. This method is very useful to change the porosity of NAA structure. Electrochemical dissolution of the oxide barrier layer of NAA has also been demonstrated by adding additional steps of re-anodization at constant current density with the current density halving with each step. This method was capable of removing the oxide barrier layer in samples fabricated by hard anodization in oxalic acid at 120 V, and the resulting structure remains on the Al substrate.[29] In order to obtain freestanding NAA membranes, the underlying metallic Al substrate is dissolved by exposing the Al side to a solution containing mercuric chloride ($HgCl_2$) until the clear membrane is visible.

The major disadvantage of mild anodization is the long fabrication time of almost three working days to prepare one NAA membrane. Pore growth rate for mild anodization is as low as 1–2 μm h^{-1}. This drawback was overcome by the invention of a new method called hard anodization by the Gösele group which can achieve pore growth rate of 50–100 μm h^{-1}.[30]

3.1. Surface Functionalization of NAA

Due to the insulating nature of NAA and its instability in acidic environment, its surface properties need to be changed by adding surface functionalities. The functionalization of the inner walls of NAA is crucial in developing biosensors to bind specific biomolecules that act as recognition elements of the analyte. It has been reported that biomolecules immobilized on NAA are more stable compared to flat surfaces.[31] Various wet chemical processes and gas phase techniques have been explored for surface modification of NAA to both improve surface properties and add surface functionalities. The numerous hydroxyl groups on NAA facilitate its chemical modification with organic molecules that introduce functional groups of interest. The most common and widely used method of surface modification adapted for biosensing applications is self-assembling organosilane molecules with desired functional groups.[32]

In this functionalization strategy, NAA is first treated in hydrogen peroxide (H_2O_2) at 70 °C for 30–60 min (hydroxylation) to activate the hydroxyl groups on the surface followed by self-assembling of the silane. The self-assembled silane can either directly bind to biomolecules, or react with a cross-linker (e.g., glutaraldehyde) to introduce the required functional groups which then allow the binding to biomolecules. If the NAA surface is coated with gold to enhance optical properties, thiolated compounds can be self-assembled to form monolayers. Alkane thiols with desired functional groups are self-assembled on gold-coated NAA spontaneously forming well-organized monolayers.[33] However, this method is not as widely used as silanization because it involves an additional step of gold deposition, whereas silanes can be self-assembled on the native NAA surface. Layer-by-layer (LBL) assembly is another surface modification technique used which involves the formation of polyelectrolyte multilayers by alternate dipping of the NAA surface in polyelectrolyte solutions with alternating charge.[34] This is a simple, inexpensive, and versatile alternative functionalization approach for NAA. Plasma polymerization has also been used to produce stable and cross-linked polymer coatings, to introduce desired functionality such as amine, hydroxyl, aldehyde, epoxy, and carboxyl groups on the surface depending on the monomer used.[35] However, this method is scarcely used for NAA surface modification despite its ability to produce stable films. This may be due to the requirement of specialized equipments and experimental setups which are not commonly available in all laboratories. Finally, metal deposition on NAA is of interest to improve its conductivity, as well as its optical, magnetic, electrochemical, and catalytic properties. Commonly used metals are gold, silver, platinum, nickel, palladium, cobalt, and titanium. Thermal deposition and sputter coating are common techniques used for depositing metals on NAA surfaces.

3.2. Properties of NAA

NAA has several innate material properties that make it highly desirable to be used as biosensing platforms for biomarker detection. A major advantage is its chemical inertness that ensures long shelf life and provides the ability to use the sensor in physiological conditions without surface degradation. Due to its porous structure, NAA has a large surface area and high aspect ratio which provide more sites for immobilization of a large amount of bioreceptors, hence making possible a high-sensitive detection. NAA membranes are excellent platforms for the detection of biomarkers in complex biological fluids due to their filtering capability to exclude large biomolecules that can cause an interference effect, and also minimizing biofouling. All these features along with the innate biocompatibility show NAA as a good biosensor interface.

Additionally, NAA has unique optical and electrochemical properties which make it an excellent platform to develop optical and electrochemical sensing systems.

Optical properties of NAA include reflectivity, transmittance, chemiluminescence, and photoluminescence (PL). PL of NAA is attributed to single ionized oxygen vacancies (F+ centers)[36] or to electrolyte impurities such as anionic species incorporated into the alumina layer during the anodization process.[37] So, the PL property of NAA strongly depends on the type of electrolyte used for anodization, the anodization voltage, and the pore diameter. Studies have shown that NAA fabricated in oxalic acid has the highest PL intensity and the corresponding PL spectrum is stable over time. It has also been shown that the PL behavior can be tuned by modifying the structural characteristics of NAA which helps in designing nanostructures with a good control over their optical properties and the performance of biosensors developed using them.[38] Santos et al. demonstrated the NAA barcode system in which the unique fingerprint of NAA was created using PL spectra based on pore geometry.[39] Briefly, the PL spectrum of NAA was converted into a barcode where each bar corresponds to an oscillation in the spectrum. The intensity of oscillation is translated to the width of each bar and the position of oscillation is translated to the position of each bar in the barcode. A range of distinct barcodes can be generated by fine tuning the geometrical structure of NAA. Highly sensitive sensors have been demonstrated based on monitoring the shift in the PL spectra prior and after infiltration of the target analyte.[40]

Interferometric reflectance spectroscopy (IRS) is the most widely used detection technique for optical NAA-based biosensors. IRS is based on the interaction between a white light beam and thin films which depends on the refractive index and thickness of the porous layer. When a white light beam interacts with NAA, it produces a Fabry–Pérot interference pattern[41] due to the interference of light rays reflected from different interfaces (air-porous alumina and porous alumina-Al substrate). Any change in the effective refractive index or thickness of a porous layer is observed as a shift in the interference pattern caused by the change in the optical thickness ($2nL$, where n is the refractive index of the media and L is the thickness of the porous layer). The Fabry–Pérot effect is defined by the equation $2nL = m\lambda$ where n is the effective refractive index of NAA, L is the thickness of the porous alumina layer, m is the order of the fringe, and λ is the wavelength of maximum constructive interference.

A comparative study between PL and IRS sensors based on NAA platforms about the sensing performance for detecting analytes: D-glucose and L-cysteine under nonspecific and specific adsorption conditions, respectively, demonstrated that the PL-based sensing platforms were more sensitive than the IRS-based ones. PL-based sensing platform showed better linearity, higher sensitivity, and lower LOD.[42]

Another optical technique used to develop NAA-based sensing systems is surface plasmon resonance (SPR). In SPR, an evanescent electromagnetic wave is produced by irradiating light on a prism, which then excites the surface plasmons on a metallic thin film coating on the glass prism at the metal–prism interface. Resonance occurs when the frequency of the incident light and that of surface electrons match. An SPR device usually consists of a setup called Kretchmann configuration in which a thin metal layer of nm thickness is deposited on a prism surface with a light source and a detector. Sensors based on SPR using NAA platforms are prepared by growing a thin NAA layer along with metal on the glass prism the plasmonic properties of which depend on the refractive index of the adjacent media. Changes of these plasmonic properties are used to monitor biorecognition events. Localized SPR (LSPR) is based on a different configuration in which light interacts with surface electrons from conductive nanoparticles smaller than the wavelength of the incident light. This interaction results in surface plasmon oscillations which depend on the refractive index of the surrounding media, nanoparticle separation, size, and geometry. Ordered arrays of metal nanoparticles, easily fabricated on NAA surfaces by metal deposition techniques, have been widely used to develop NAA-LSPR sensing devices.[33,43]

NAA modified with metals such as gold and silver by sputtering or evaporative methods has been demonstrated to show excellent surface-enhanced Raman scattering (SERS) effects due to its highly organized nanostructure. This has been used as a highly sensitive optical technique which is based on an enhancement in Raman scattering when target molecules are adsorbed on the metal surface with nanometric surface roughness, known as "hot spots" or "hot junctions." Strong Raman signal enhancements of up to the order of 10^6 have been demonstrated using NAA modified using gold or silver nanoparticles for detection of trace amounts of analytes such as 2,5-dinitrotoluene,[44] *p*-aminothiophenol,[45] and 4-mercaptopyridine.[46] Nanowires and nanotubes embedded inside NAA have also been used to develop SERS biosensors.[47] However, this technique has not been used to develop biosensors for detection of any biomarkers to the best of our knowledge.

Electrochemical impedance spectroscopy (EIS), amperometry, voltammetry, and capacitance are the various techniques used for developing NAA-based electrochemical biosensing platforms. Our literature survey shows that there are almost three times as many papers on electrochemical biosensors based on NAA compared to optical biosensors despite the remarkable optical properties of NAA described above. One possible reason is that electrochemical techniques can be easily miniaturized and translated into a POC device by integrating them into microchips using microfabrication methods. Electrodes modified with NAA membranes have been used to develop electrochemical biosensors for the detection of a variety of biomarkers. When the barrier oxide layer at the pore bottom of NAA is removed, the resulting nanochannels can conduct ions/current through them. This opens up the possibility to use NAA for monitoring binding events within the pores by detecting changes in conductivity/current into the pore channel. In the case of impedimetric biosensors, the electrical characteristics of NAA membrane-modified electrodes are represented by an equivalent circuit model which allows the measurement of the changes in impedance or conductance caused by biorecognition events within the nanochannels. NAA-modified electrodes have also been widely used as voltammetric biosensors for various analytes. These biosensors rely on the nanochannel blockage caused by biorecognition events which is measured by the change in the oxidation/reduction current of a redox species added in solution. These techniques together with key examples will be detailed in the next section.

4. NAA-Based Biosensing Platforms for Biomarker Detection

4.1. Pathogen Detection

Pathogen detection is crucial to prevent and identify several health-related problems. Traditional pathogen detection methods such as PCR, culture, and colony counting methods are slow, often too slow for the purpose, and thus rapid detection methods are required. In 2008, Lazcka et al. compared biosensors and the traditional methods used for pathogen detection.[48] They concluded that although electrochemical biosensors are much easier to use and to integrate into microdevices, they do not reach the detection levels of the traditional methods. The authors also remarked that optical detection techniques provide higher sensitivity, but the cost and complexity associated make them unfavorable to the desired applications. So there is a need for detection systems that can reach a detection level comparable to the traditional ones which is between 10 and 100 CFU mL^{-1} and allow their integration to develop POC devices.

NAA provides a high surface area to accommodate biorecognition events within the pores, and make it an excellent platform for pathogen detection. Several reports use NAA as electrochemical sensing platform for pathogen detection with high sensitivity and desired detection levels. These NAA-based pathogen sensing systems have been developed against a range of pathogens such as West Nile Virus (WNV),[49] *E. coli* O157:H7,[50] DENV,[51] *Staphylococcus aureus* (*S. aureus*),[50c] and *Legionella pneumophila*.[52]

Toh's group has exploited the use of NAA membrane-coated electrodes for the electrochemical detection of several pathogens such as WNV,[49] DENV,[51a–c,e] *E. coli*,[50b] and *Legionella pneumophila*.[52] This research group developed a method to fabricate homemade electrodes integrated with NAA using readily available lab consumables. Pt wires were embedded in micropipette tips and sputter coated with high-purity Al. Al-coated tips were etched using the technique developed by the same group known as surface contact anodization.[53] The applicability of these membrane-modified electrodes was validated by quantifying the antigen–antibody binding within the pores via the change in Faradaic current of ferrocenemethanol, a redox species added in solution. The immuno-complex formed by the binding of the target analyte to the antibody immobilized within the pores limits the diffusion of ferrocenemethanol toward the underlying Pt, causing a reduction in the Faradaic current which is measured using differential pulse voltammetry (DPV). The biosensor based on anti-glucose oxidase (GOx) IgG as the capture probe showed a very low limit of detection (LOD) of 100 ng L^{-1} of GOx and selectivity toward GOx protein in the presence of glucothione S-transferase.[54]

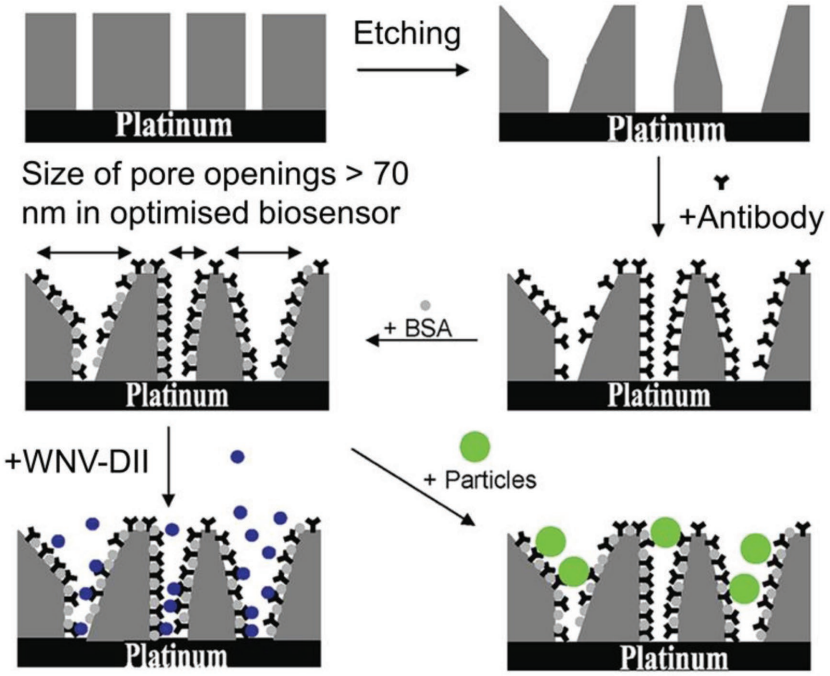

Figure 2. Scheme of operation for the membrane-based electrochemical nanobiosensor for the detection of the WNV-DIII protein and the WNV particle. Reproduced with permission.[49] Copyright 2009, American Chemical Society.

Later, the same technology was applied to detect WNV particles and WNV protein domain III (WNV-DIII) using WNV-DIII IgG M as the biorecognition probe immobilized within the NAA pores.[49] **Figure 2** shows the NAA-modified electrode fabrication and sensing strategy developed by this group. A low detection time of 30 min, and a extremely low LOD of 4 pg mL^{-1} and ≈2 viral particles per 100 mL, were achieved, being much more sensitive than conventional methods such as PCR.

DENV is a mosquito borne virus which causes Dengue fever or severe forms such as Dengue hemorrhagic fever (DHF) and Dengue shock syndrome (DSS). Dengue is caused by one of the four serotypes of DENV (DENV1-DENV4).[55] Dengue is more prevalent in tropical and subtropical regions of the world and over 2.5 billion people of the world population are at risk for Dengue. For timely and appropriate treatment of the disease, rapid diagnosis platforms are therefore essential. The above sensing concept employed by Toh's group was also used for the detection of DENV[51a,e] using two approaches. In the first one, Dengue type 2 virus (DENV-2) was detected by immobilizing anti-DENV-2 monoclonal antibody on NAA, achieving a LOD as low as 1 PFU mL^{-1}. This sensor was highly selective toward DENV-2, showing no cross reaction with nonspecific viruses such as Chikungunya virus, WNV, and DENV-3.[51a] This is the first report of an electrochemical biosensor for the detection of DENV-2 and thus a first approach toward the development of a POC test device for first hand diagnosis of Dengue fever. The second approach was based on the detection of a 31-mer specific sequence of the DENV genome on NAA nanochannels modified with a complimentary ssDNA capture probe.[51e] In this approach, ferrocyanide ($[Fe(CN)_6]^{4-}$) was used as a redox species whose mass transfer toward Pt electrode was partially blocked when the target DNA molecule bound to the capture probe immobilized inside the nanochannels. This NAA sensor showed a LOD of 10^{-12} M with a wide linear range of six orders of magnitude and high specificity down to one base mismatch. The high aspect ratio and surface area of the NAA-modified electrode allow high probe loading which helps in achieving a low LOD. Further to this, EIS was also used as a detection technique using the homemade NAA membrane-coated electrodes for detection of DENV-2.[51b,c] EIS is an ideal technique to be used with NAA membranes, because the electrical characteristics of the NAA sensing platform can be easily adjusted to an equivalent electric circuit in a way that changes in pore resistance caused by the recognition events are used to quantify the analyte of interest. A linear increase in pore resistance was observed toward increasing concentrations of ssDNA related to DENV-2 with a LOD of 2.7×10^{-12} M and being selective toward even single base mismatches.[51b] DENV-2 detection was also achieved using EIS as measuring technique and an immuno-based approach, with DENV-2 IgG as the capture probe instead of ssDNA within NAA nanopore channels, obtaining a linear range of 1–900 PFU mL^{-1}.[51c]

Another NAA membrane-based biosensor for the detection of DENV-2 was reported by Peh et al., using NAA commercial membranes (Anodisc, 200 nm pore size, 60 µm thickness) coated at both sides with sub-micrometer layers of Pt to act as both working and counter electrodes. 2H2 antibodies were used as capture probes which were physically adsorbed, and BSA was added to block any available sites to prevent nonspecific adsorption. Detection was based on resistive pulse sensing method, where binding events cause a reduction in ion current resulting in a downward current pulse which causes an increase in resistance in the impedance measurement. Changes in pore resistance were measured using EIS, affording a very low LOD of 0.23 and 0.71 PFU mL^{-1} for DENV-2 and DENV-3, respectively, with a detection time of 40 min.[51d]

E. coli is the most relevant and commonly targeted biomarker which indicates food and water contamination that can cause various diseases such as diarrhea, kidney failure, and urinary tract infections. NAA membrane-based sensors have been developed using anti-*E. coli* antibodies as biorecognition probes, which selectively capture *E. coli* on the membrane pore surface, blocking the diffusion of redox species (ferrocenemethanol) toward the underlying Pt electrode.[50b] Blocking of nanochannels due to formation of immuno complexes on the surface results in a reduction in Faradaic current, measured using cyclic voltammetry. A LOD of 22 CFU mL^{-1} was achieved in this study with a linear response from 10 to 10^6 CFU mL^{-1}. *E. coli* cell viability was also studied by measuring the activity of the redox enzyme D-glucose dehydrogenase (GDH) on the outer surface of the cytoplasmic membrane of the *E. coli* cells captured on the biosensor surface. The enzymatic activity was measured using linear sweep voltammetric response of viable but nonculturable and dead cells upon the addition of glucose, as enzymatic substrate, and the neutral redox species ferrocenemethanol as electron mediator. GDH can oxidase D-glucose to D-gluconolactone using ferrocenemethanol as an artificial electron acceptor. An increase in current is used as an indicator of the viability of cells which is attributed to the redox cycling of ferrocenemethanol by active GDH enzyme on the outer surface of cytoplasmic membrane, in the presence of glucose.

Joung et al. recently developed an impedimetric immunosensor for detection of *E. coli* O157:H7 using commercial NAA membranes (Whatman Anodisc).[56] NAA membranes were modified with hyaluronic acid (HA) to introduce carboxylic groups used for further covalent immobilization of anti-*E. coli* antibodies. The immunosensor consisted of a polydimethylsiloxane (PDMS) chamber divided into an upper and a lower subchamber by an NAA membrane. As the bacteria bind to the membrane, the flow of current through the pores is limited and thus the pore resistance increases. This was measured as a change in impedance, showing a linear relationship with the concentration of *E. coli*. The system worked efficiently in complex media like milk, with a LOD of 84 CFU mL^{-1}.

The integration of sensors into microdevices is key to develop POC devices. Tan et al. reported the integration of an NAA membrane-based impedimetric sensor into microfluidic chips for the detection of *E. coli* O157:H7 and *S. aureus*.[50c] In this work, antibodies against both bacteria were covalently immobilized on membranes previously functionalized with monolayers of epoxy silane. The antibody-modified NAA membranes were then integrated into a PDMS-based microfluidic device which had an upper and a lower compartment. Bacteria were introduced into the upper chamber and, upon binding with the corresponding antibodies, the electrolyte current was blocked which was monitored as a change in impedance. Rapid bacteria detection within 2 h with a LOD of 10^2 CFU mL^{-1} was achieved. The same group recently developed a platform based on the same sensing principle for the simultaneous detection of *E. coli* O157:H7 and *S. aureus* with a linear detection range from 10^2 to 10^5 CFU mL^{-1} and a LOD around 10^2 CFU mL^{-1}.[57] The sensing platform consisted of two NAA membranes (100 nm pore size, 60 µm thickness) modified with anti-*E. coli* 0157:H7 antibody and anti-*S. aureus* antibody, respectively, which were then integrated into a PDMS chip via UV-assisted bonding. NAA membranes were first self-assembled with silane-PEG-NHS linkers to allow the covalent immobilization of probe antibodies. The PEG monolayer significantly reduced nonspecific bacteria binding. Sensing was based on pore-blocking which limits the flow of electrolyte through the nanopores which was measured as an increase in impedance amplitude signal after the bacteria was captured on the surface. The device was composed of one common upper chamber and two bottom chambers. Two independent sensing elements were formed by placing the specific antibody functionalized membranes between the upper chamber and two bottom chambers which acted as *E. coli* 0157:H7 and *S. aureus* sensing elements, respectively. The bottom chambers were connected to two separate Pt electrodes which act as the working electrodes and one Pt electrode was inserted in the upper chamber that acts as a reference electrode. In this way, each bottom chamber works independently for specific bacteria detection. **Figure 3** shows the sensing mechanism and simultaneous detection strategy of the microfluidic device integrated with functionalized NAA membranes. Tests with pure and mixed bacteria samples demonstrated that the device can perform simultaneous detection of both types of bacteria in a highly specific and sensitive manner.

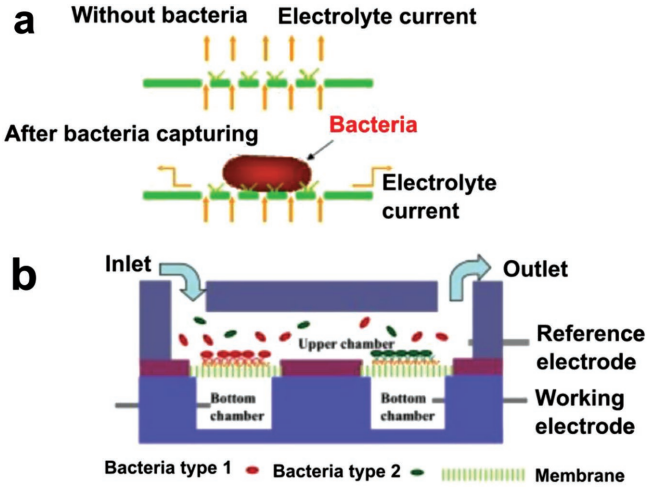

Figure 3. a) The bacteria sensing mechanism of an NAA membrane via impedance spectrum. b) Principle of simultaneous detection for two types of bacteria using a microfluidic device integrated with NAA membranes. Reproduced with permission.[57] Copyright 2015, Elsevier.

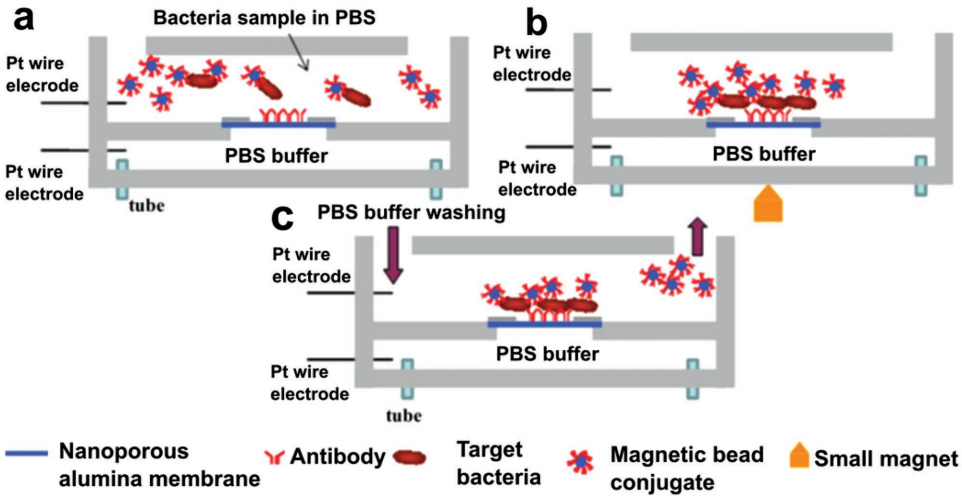

Figure 4. Schematic diagram for biofunctional magnetic bead concentration of bacteria cells in a biochip. a) Magnetic beads were bound to bacteria cells via antibody–antigen interaction. b) Bacteria cells were concentrated in a small region by applying an external point magnetic field and captured by the antibody immobilized on nanoporous membrane. c) The external magnetic field was released and unbounded magnetic beads were washed away. Reproduced with permission.[50a] Copyright 2012, Elsevier.

Chan et al. exploited the use of magnetic beads for concentrating *E. coli* O157:H7 bacterial cells to enhance the sensitivity and lower the LOD of an electrochemical NAA membrane-based immunosensor.[50a] Biofunctional magnetic particles conjugated with anti-*E. coli* O157:H7 antibodies were used to capture bacterial cells. An NAA membrane was modified with anti-*E. coli* antibodies by covalent immobilization onto a self-assembled monolayer of silane-PEG-NHS and integrated into a PDMS microfluidic chip. The NAA membrane separated the flow chamber of the microchip into two compartments, each one with a Pt wire to allow impedance measurements. After magnetic pre-concentration of *E. coli* O157:H7 cells, the magnetic particle conjugated *E. coli* O157:H7 were captured on the antibody-modified NAA membrane to form a sandwich complex. Binding events were measured as an increase in impedance. Schematic of the sensing technique is given in **Figure 4**. The use of magnetic beads significantly enhanced the sensitivity of the sensor with a LOD as low as 10 CFU mL^{-1}.

Legionella pneumophila is a lethal pathogen that causes a severe form of pneumonia called Legionnaires' disease. It is crucial to have a rapid diagnosis of this disease for patient survival. An electrochemical NAA-based biosensor for ultrasensitive detection of this pathogen was developed by Toh's group using 5-aminated DNA probes immobilized within the nanochannels of NAA. Hybridization of target DNA analyte of *Legionella sp*. to the probe DNA was measured as a reduction in Faradaic current of redox species $[Fe(CN)_6]^{4-}$ due to the pore-blocking effect. This was measured by means of DPV as a decrease in oxidation current. A label-free detection of analyte was achieved with a LOD of 3.1×10^{-13} M.[52]

4.2. Small Molecule Detection

The term small molecule refers to molecules that have a low molecular weight (<900 Da) that include lipids, monosaccharides, second messengers, other natural products and metabolites, as well as drugs and xenobiotics.[58] NAA-based sensors have been developed for small molecule biomarkers such as glucose,[39,59] cholesterol,[60] urea,[61] sucrose,[62] biotin,[63] and dopamine.[64] These sensors relied on electrochemical, optical, and piezoelectric transduction techniques.

Rapid and reliable sensing platforms for glucose detection are always on high demand. The most common biosensors for glucose quantification are based on the amperometric detection of H_2O_2 on GOx-modified electrodes.[59a] The current intensity measured is directly related to the glucose concentration. In such sensors, maintaining the activity of enzymes over time is a big challenge. With the right choice of substrate environment, this issue can be solved. Materials with nanoconfinement protect the enzymes immobilized within them and prevent them from losing their activity. NAA membranes are thus a suitable matrix for immobilizing the enzymes within their nanochannels potentially keeping the enzymes stable and offering improved sensing performance. Li et al. constructed an ultrasensitive flow channel biosensor based on NAA membranes for glucose detection.[59a] GOx was covalently immobilized on NAA nanochannels using aminosilane and glutaraldehyde coupling chemistry. One side of the NAA membrane was Pt sputter coated to act as the working electrode. When glucose flowed through the nanochannels containing GOx, enzymatic conversion into H_2O_2 occurred which was amperometrically detected at the Pt side of the membrane. This system showed an improved efficiency in detecting H_2O_2 and retained the activity of GOx due to the presence of nanochannels which resulted in a high performing glucose sensor with a LOD of 0.01 M and sensitivity of 86.63 μA mM^{-1} cm^{-2}. The authors found that the flow rate is a key performing factor, showing an increase in the sensitivity at high flow rates.

In another strategy by Xian et al., NAA membrane was used as a template for the ordered deposition of Prussian Blue (PB), obtaining a nanoelectrode array.[59c] First, gold was sputtered on one side of the membrane and attached to a glassy carbon electrode (GCE). PB was then electrodeposited on the membrane

pores followed by immobilization of GOx on the nanoelectrode array. Glucose quantification was carried out by electrochemical detection of enzymatically liberated H_2O_2 and a LOD of 1×10^{-6} M was achieved.

Maghsoodi et al. developed a novel carbon nanotube (CNT)/alumina electrode with high electrical conductivity, biocompatibility, and stability[59b] for glucose detection. CNTs were grown on a Fe/MgO sputter coated alumina surface by chemical vapor deposition of methane at 950 °C for 15 min. GOx was immobilized on the CNT which acted as the conducting electrode. The sensor showed a linear response between 12 and 62×10^{-6} M glucose with a LOD and sensitivity of 0.1×10^{-6} M and 635 μA mM^{-1} cm^{-2}, respectively.

Cholesterol detection is gaining more and more attention in day-to-day life as more and more people are prone to CVDs with changing lifestyles. Total plasma cholesterol level must be ideally less than 5.2×10^{-3} M (200 mg dL^{-1}) and if the level is greater than 6.2×10^{-3} M, there is a high risk of poor cardiovascular conditions such as atherosclerosis, hypertension, myocardial and cerebral infarction, and coronary heart diseases.[65] LDL-cholesterol has been detected using home-made NAA membrane-modified rhodium-graphite screen-printed electrodes (SPEs) as an enzymatic sensor with cytochrome P450scc as biorecognition element.[60b] P450scc enzyme was immobilized using poly-L-lysine (PLL) as an intermediate structure. Briefly, NAA nanochannels were first coated with PLL by vacuum deposition. Then the P450scc cytochrome was added over the PLL covered surface by solution casting and then dried overnight at 4 °C. Negatively charged P450cc interacts with the positive charges of PLL to confine it within the nanochannels. Detection of LDL-cholesterol in clinical range was achieved using cyclic voltammetry as the detection technique. Electrochemical measurements were carried out in 10×10^{-3} M phosphate buffer at pH 7.4. NAA-PLL modified electrodes showed no redox peaks, while immobilization of P450 resulted in a well-defined redox peak attributed to the electrochemical reaction of the heme-redox-active metal complex of P450. Interaction of LDL-cholesterol with the P450 immobilized on the NAA-PLL modified electrode resulted in an enhancement in the redox peak due to the enzymatic oxidation of the substrate by P450 scc. This electron transfer during the catalytic activity of immobilized enzyme toward analyte was used as the analytical signal.

A novel nonenzymatic sensor was reported for the detection of cholesterol using porous tubular silver (Ag) nanoparticles prepared using NAA as a template.[60a] The porous Ag nanoparticles were prepared by a simple method. Initially, NAA template was pre-treated with CdS which is followed by electrodeposition of Ag into the cadmium sulfide (CdS)-modified NAA template, and subsequent removal of CdS. Porous Ag nanoparticles were used to modify a GCE and detection of cholesterol was carried out using cyclic voltammetry as the detection technique. CVs of Ag nanoparticle modified GCE in 0.1 M NaOH in the absence of cholesterol showed no redox peak while with the addition of cholesterol, there was a dramatic change in the shape of CV with an increase in oxidation current, indicating the electrocatalytic nature of the tubular silver nanoparticles to the oxidation of cholesterol. This sensor had a linear response range of 2.8×10^{-4} to 3.3×10^{-2} M and LOD of 1.8×10^{-4} M.

Kisner et al. fabricated an ion-sensitive field effect transistor (ISFETs) with an NAA layer at the gate for the detection of the neurotransmitter dopamine.[64] Use of ISFETs as biosensors are gaining popularity since they can be used as miniaturized biosensors for POC applications.[66] Detection of analytes using ISFETs is based on the variation in surface potential of the gate of the devices when specific binding to the gate occurs, which leads to a change in electrical current between source and drain. The enzyme tyrosinase was immobilized on the NAA layer. Tyrosinase oxidizes dopamine into *o*-dopaminequinone with a release of two protons at the transistor gate. This reaction alters the surface potential and causes a change in electrical current in the conductive channel. The high surface area of NAA plays a key role in the ionic conductance of the surface and enhances the sensitivity of the system. Dopamine detection at the physiological concentration was achieved from 10×10^{-6} to 2×10^{-6} M.

Santos et al. developed an optical barcode system using PL spectra of NAA in the UV–vis range in which each bar corresponded to an oscillation in the PL spectrum.[39] The width and position of the bar correspond to the intensity and position of each oscillation. They demonstrated that by controlling pore geometry (pore length and diameter) of NAA via control of the anodization parameters and pore widening time, the effective medium of the material can be altered to design PL spectra with desired intensity, position, and number of oscillations. This results in a wide range of distinct barcodes which can be chosen to suit each sensing purpose. The sensor was tested for the detection of glucose as a model system to demonstrate the sensing responsiveness of NAA using this technique. This new encoding system can be used for developing smart optical biosensors for biomarker detection.

An SPR-NAA biosensor showed the ability to quantify sucrose using invertase enzyme immobilized within the pores.[62] Invertase enzyme was immobilized by physical adsorption on NAA (65 nm pore diameter) previously cleaned by dipping and sonicating in isopropyl alcohol (IPA). Activity of the enzyme inside the pores was studied in a flow cell where substrate (sucrose) is made to flow and the interaction with sucrose is detected by SPR.

Ryser's group recently reported a glucose sensor based on the viscosity variation of a sensitive liquid containing dextran and concanavalin A (ConA). Sensing is based on the competitive affinity of glucose and dextran to ConA which is a saccharide binding protein.[59d,67] In the absence of glucose, dextran molecules are cross-linked by binding to ConA in the sensitive solution which renders it a high viscosity. As the glucose concentration in the solution increases, dextran molecules are replaced by glucose molecules which bind to ConA, weakening the ConA-dextran network and reducing the viscosity of the solution. The sensor comprises two microchambers filled with this glucose sensitive solution that communicate through a microchannel and an NAA membrane (**Figure 5**). The membrane allows the confinement of this solution inside the system, prevents large molecules to enter, and allows a smooth passage of glucose into the chamber. Each chamber has a flexible piezoelectric diaphragm, one that deflects under a voltage (actuating diaphragm) and the other one generates voltage under some pressure load (sensing diaphragm). A voltage applied

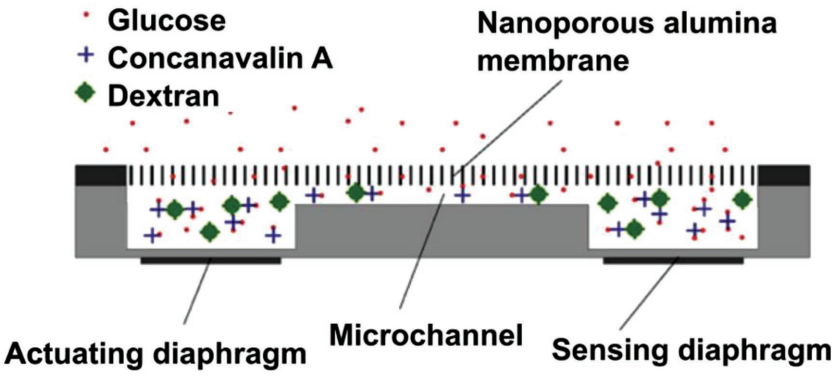

Figure 5. Schematic illustration of NAA membrane in the glucose affinity sensor. Large analytes (ConA and dextran) are confined in the sensor while glucose permeates through the membrane. Reproduced with permission.[67] Copyright 2012, Elsevier.

at the actuating diaphragm causes the fluid to move through the microchannel due to the deflection of the diaphragm. This movement, which depends on the fluid resistance, causes a deflection at the sensing diaphragm which in turn induces a voltage. The sensor showed excellent response in blood serum with physiological blood glucose concentrations between 2 and 20×10^{-3} M, and a very short response time of around 13 min.

Yang et al. used single enzyme nanoparticles (SENs) immobilized on NAA membranes to develop a novel ultrasensitive piezoelectric urea biosensor.[61b] Maintaining the activity of enzymes in biosensors has always been a significant challenge. Encapsulation of single enzyme molecules is a way to retain the enzyme activity and provide high stability to enzyme sensors. SENs synthesized according to the method described elsewhere[68] were immobilized onto the NAA membranes by immersing in a pH 6.5 phosphate-buffered saline (PBS) solution containing 1 mg mL^{-1} SENs for 1.5 h and then washing with water. Then 10 µL of 1% chitosan and 1% acetic acid were spread on the NAA membranes and left overnight for coating. The authors studied the enzymatic activity and stability of urease immobilized on NAA membranes depending on pore geometry.[61a] Results revealed that large pores increase the enzymatic activity and small pores enhance the enzymatic stability. The sensor with highest enzymatic activity had a pore diameter of 200 nm and pore length of 105 µm. It showed a linear range for urea detection from 0.08×10^{-6} to 1×10^{-3} M, short response time (12 s), high stability, excellent selectivity, and low LOD (0.05×10^{-6} M).

4.3. Protein Detection

Several electrochemical and optical sensors based on NAA have been developed in the recent years for protein detection. Merkoci's group has developed several NAA nanochannel-based electrochemical biosensing systems[32,69] where NAA membranes are combined with SPE to fabricate nanostructured electrodes. The detection is based on pore-blocking where blockage in diffusion of a redox species toward the electrode due to binding events is monitored by changes in the current intensity measured by DPV. Immunodetection of proteins within the nanochannels is achieved with high sensitivity and at the same time the membrane acts as a filter and prevents the diffusion of large biomolecules from complex media like blood to minimize matrix effects. Binding of human IgG inside the channels modified with anti-human IgG antibodies was initially demonstrated with a LOD of 98 µg mL^{-1} of human IgG.[32] Later this system was combined with 80 nm Au nanoparticles (Au NPs) tags as blocking enhancers in an immune sandwich assay where secondary immunoreaction was carried out using AuNP modified with secondary antibodies. AuNP tags act as blocking agents to amplify the analytical signal (**Figure 6**) and this lowered the LOD to 2 µg mL^{-1}.[69a] Further signal enhancement was obtained upon silver deposition catalyzed by the AuNP used as labels, lowering the LOD further to 50 ng mL^{-1}. A similar platform was used for the detection of CA 15-3. CA15-3 is considered a particularly important biomarker in breast cancer. While the normal level of CA15-3 is less than 30 U mL^{-1}, women with cancer can have levels as high as 100 U mL^{-1}. Detection of CA15-3 allows physicians to monitor the treatment and progression of breast cancer. Immunodetection of CA15-3 in both buffer and whole blood was demonstrated giving a LOD of 52 U mL^{-1}.[69a]

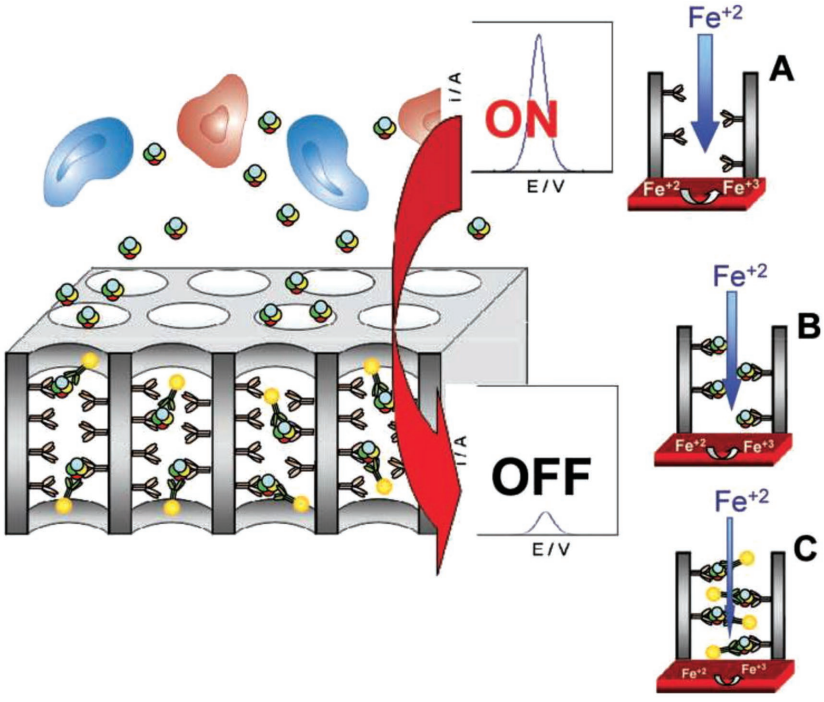

Figure 6. Protein sensing technology using NAA membrane by pore blocking. The cells in the blood sample remain outside the pores and the proteins enter the porous layer and react with the capture antibodies. Reproduced with permission.[69a]

Thrombin detection in whole blood has been achieved using an aptamer-modified nanochannel system using the same detection technique with a AuNP-modified secondary antibody for a mixed sandwich assay, achieving a LOD of 1.8 ng mL^{-1}.[69b] This platform showed the potential for protein detection in complex samples with no sample preparation, high robustness, selectivity, and sensitivity. Recently, the same authors have greatly enhanced the sensitivity of this system by using polyvinylpyrrolidone-protected Prussian Blue nanoparticles (PBNP) (4 nm diameter) as redox species instead of the ionic-based indicators like $[Fe(CN)_6]^{4-/3-}$ previously used.[70] The larger size of PBNPs than ionic indicators increases the steric hindrance, significantly improving the LOD from 200 μg mL^{-1} to 34 pg mL^{-1} of human IgG. Using the same sensing approach, the detection of the cancer biomarker parathyroid hormone-related protein (PTHrP) was achieved with a LOD of 50 ng mL^{-1}.

Ye et al. reported an impedance sensor for the detection of Botulinum neurotoxin A (BoNT) using an NAA membrane modified with synaptosomal associated protein 25 (SNAP-25) via epoxy silane linker molecules,[71] integrated in a PDMS chamber. BoNT has specific endopeptidase activity toward SNAP-25 and this cleavage activity was monitored by measuring changes in impedance. In the absence of BoNT, SNAP-25 blocked the pores. In the presence of BoNT, its activity cleaved the immobilized SNAP-25, reducing the blocking effect and thus decreasing pore resistance. Changes in pore resistance were measured to quantify BoNT with a LOD of 500×10^{-12} M and a response time of 25 min.

As mentioned earlier, NAA can be easily modified to form highly ordered arrays of metallic NPs (nanocaps) on its top surface by techniques such as metal evaporation, self-assembly methods, or sputter coating. Such structures have the potential to be used as substrates for LSPR devices. A highly sensitive LSPR sensor for the detection of antigen–antibody interaction has been reported.[33] Shifts in LSPR signal due to the capture of protein on the surface were observed for the detection of C-reactive protein (CRP) using Au-capped NAA.[33,43c] Another sensitive LSPR sensing system was developed using NAA on an Al substrate with gold plasmonic nanoparticles on the top surface to study biomolecular interactions. The proposed system was shown as a proof-of-concept for the detection of protein biomarkers.[43b]

Real-time label-free detection of anti-sheep IgG, with minimal nonspecific binding, was demonstrated on an IgG-protein A-modified NAA substrate using IRS to measure changes in refractive index.[41a] In another study using interferometry as the detection technique, the effect of pore geometry of NAA on sensitivity for the detection of β-galactosidase using prolinker A as a bio-probe within the pores was investigated.[72] The optimal pore geometry chosen for best sensing performance was NAA film with 30 nm pore diameter, 1.74 μm pore length, and 110 nm interpore interval. Using this pore geometry, a linear relationship was observed between effective optical thickness (EOT) changes caused by β-galactosidase binding and β-galactosidase concentration with a LOD of 70 ng mL^{-1} which is 200 times more sensitive than previously reported similar porous silicon-based sensors. There is scope for further enhancement of sensitivity by finely tuning the pore depth and pore distribution.

A smart PL enzymatic sensor was developed by Santos et al. for the detection of trypsin.[40a] Changes in EOT of PL spectra were monitored as a result of protein binding inside the pores. NAA geometry was tuned to optimize the sensor performance and the most optimum sensing response was obtained for NAA with 34 nm pore diameter and 5.3 μm pore length. Similar studies done by Jia et al. showed that the capture of proteins (morin, trypsin, and human serum albumin) on NAA can be detected by monitoring the shift in PL spectrum.[40b]

4.4. Nucleic Acid Detection

Nucleic acid detection is important in clinical microbiology laboratories mainly for diagnosis of infectious diseases,[73] genetic diagnostics, and virus detection. Currently, the detection methods include amplification strategies like PCR and culture methods, fluorescence assays, and immunoassays. Limitations of these methods include high cost, complex instrumentation, and long waiting time. Smirnov's group demonstrated for the first time an electrochemical NAA-based sensing system for detecting DNA hybridization within the pores.[74] NAA was modified by covalently linking a ssDNA capture probe on its surface, complementary to the target DNA sequences. Detection was based on partial blockage of the pores upon hybridization which limited the diffusion of electroactive species added in solution toward the electrode. Cyclic voltammetry, impedance spectroscopy, and direct current conductance were used as detection techniques in this study. The importance of pore size was also demonstrated in their study where the effect was observed with 20 nm pores and is absent for 200 nm pores. A similar sensing concept was demonstrated by Rai et al. by immobilizing a 5-aminated ssDNA capture probe on NAA membranes and monitoring the hybridization of the complementary target DNA, achieving a LOD of 3.1×20^{-13} M.[52]

Later, Merkoci's group demonstrated an enhancement in sensitivity of similar sensing assays using nanoparticle tags.[69a] DNA detection with enhanced sensitivity was achieved using 20 nm AuNP tags which cause an additional blocking effect, measured as a decrease in the current intensity produced by the oxidation of the electroactive species added in solution. The authors were able to achieve a LOD of 42 ng mL^{-1}.[75] Another label-free sensing strategy was reported by Li et al. using morpholino (DNA neutral analogue)-modified NAA nanochannels which gave a LOD of 0.1×10^{-9} M.[76] Interaction between DNA-morpholino resulted in a negatively charged complex which hindered the diffusion of redox species $[Fe(CN)_6]^{3-}$ due to the electrostatic effect, and was measured by monitoring the current response of the probe ions at the electrode surface.

Single nucleotide polymorphisms (SNPs) are the most common type of gene variation among people which is a variation at a single nucleotide in a DNA sequence (alleles). SNPs affect physical appearance, how an individual respond to drugs/treatments and how diseases are developed. They are also associated to complex diseases such as heart disease, diabetes, many genetic diseases, and cancers. They can also give an indication of how an individual can develop certain diseases. Hence, detection of SNPs is really of interest for disease diagnosis, prevention, and in personalized medicine. Allele-specific PCR and electrophoresis are the conventional methods to identify SNPs which has limitations such as complexity, long analysis, time and cost.

Gao et al. reported a DNA/morpholino duplex functionalized NAA nanochannel system for highly sensitive and label-free detection of SNPs by monitoring $[Fe(CN)_6]^{4-}$ probe diffusion flux.[77] The detection is based on the competition of the target DNA for its binding to morpholino in front of the DNA already bound in the DNA/morpholino duplex which results in a change in surface charge. This affects the diffusion flux of redox species due to electrostatic interactions. This system was able to detect single base or two base mismatched sequences and also the location of mismatched bases. The authors demonstrated the detection of SNPs in the PML/RARα fusion gene which is a biomarker of acute promyelocytic leukemia (APL).

More recently, Yang's group reported an impedance sensor for DNA detection using NAA with covalently immobilized ssDNA probe within the pores.[78] Pore blockage due to DNA hybridization was measured as an increase in pore resistance using impedance spectroscopy. The blockage signal was further enhanced using AuNPs tags and catalytic silver deposition, obtaining a LOD of 50×10^{-12} M.

A similar sensing strategy for DNA detection by impedance spectroscopy was reported using microfabricated thin film NAA membranes by monitoring increase in impedance within pores during DNA hybridization. NAA membranes were coated with silica nanoparticles by dipping the chips in a solution containing 20 wt% silica nanoparticles (10–20 nm diameter) to increase the total surface area. The ssDNA capture probe was immobilized in the membrane by functionalizing the membranes initially with (3-glycidoxypropyl) trimethoxysilane (GMPS) and then adding ssDNA oligomers to functionalized membranes. Wafer-scale fabrication of NAA with controllable pore geometry was demonstrated (**Figure 7**) which is a promising platform for developing integrable and portable biosensing devices that can serve as POC devices in clinical setups. A detection limit of 12.5×10^{-9} M in PBS solution was achieved using this sensor.[79]

Pan and Rothberg reported an NAA-based IRS sensor for label-free detection of complementary DNA with a LOD of 2 nmol cm^{-2} in a 0.5 cm^2 probe area.[80] Gold-capped NAA nanostructures showed to be efficient in pM level detection of untagged target oligonucleotides using LSPR combined with interferometry as detection techniques. An Au layer was deposited by thermal evaporation on NAA films fabricated by two-step anodization which resulted in a "caplike" Au layer on the surface (**Figure 8**). Optical patterns formed from this structure were highly sensitive to changes in EOT measured using IRS and LSPR techniques.[43a]

A unique biosensor was reported by Feng et al. that was comprised of nanotubes (NTs) modified by gradient of different quantum dots (QDs), which was used for detecting DNA hybridization.[59c] QDs were used as fluorescence resonance energy transfer (FRET) donors where amplification of the detected fluorescence signal was achieved by making use of FRET. Initially, ordered NAA membranes (400 nm diameter, 100 µm depth) were coated with 3-aminopropyl silane (3-APS) which is positively charged, and then cationic and anionic polyelectrolyte dendrimers were alternatively deposited to

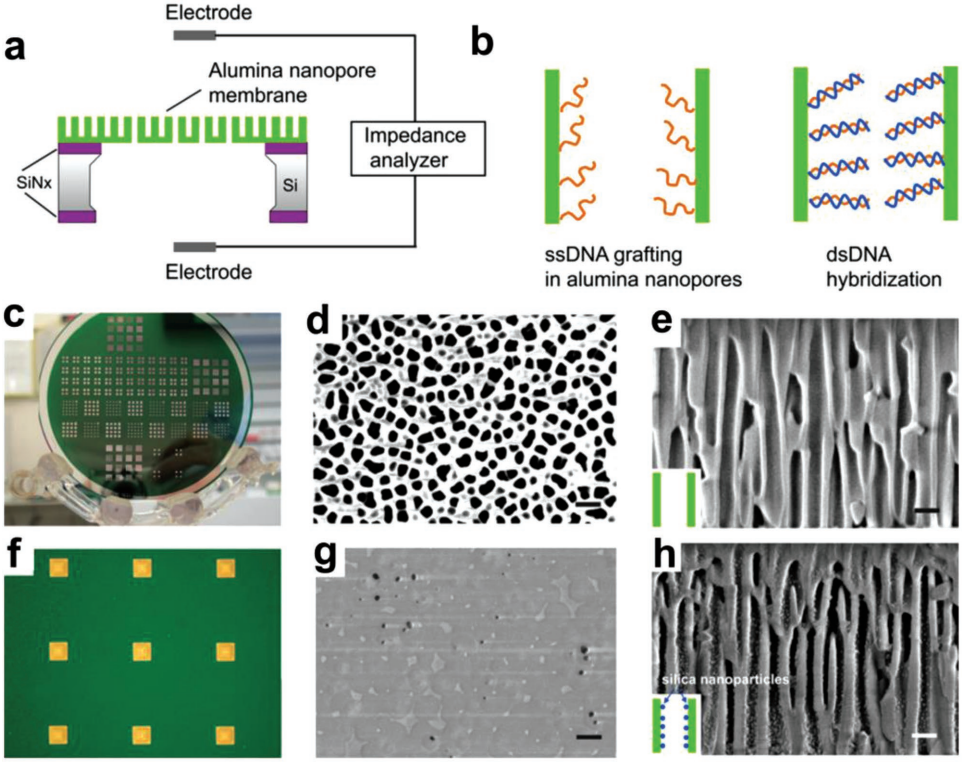

Figure 7. a) Schematic of an impedance sensor based on microfabricated NAA membrane. b) Schematic of the nanopore structure before and after DNA hybridization, c) photograph of microfabricated NAA membranes with various configurations, d) SEM image of top side of the membrane, e) SEM image of the cross-section of NAA membrane, f) optical image of an array of NAA membranes, g) SEM image of the bottom side of membrane, and h) SEM image of the cross-section image of silica nanoparticle (20 nm) coated NAA membrane. Scale bar: 200 nm. Reproduced with permission.[79] Copyright 2015, Elsevier.

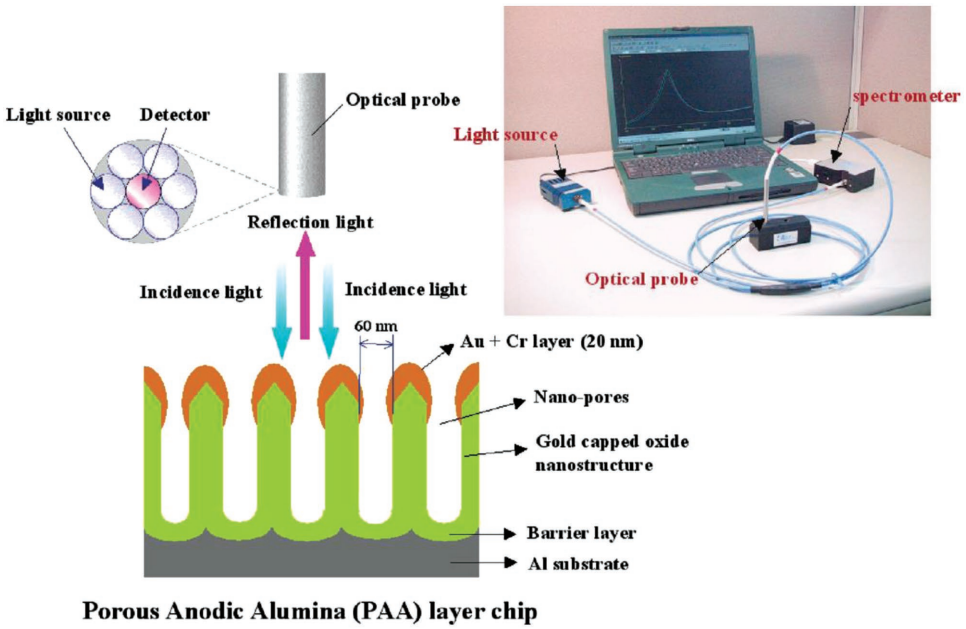

Figure 8. Experimental setup and construction of LSPR and IRS-based label-free DNA optical biosensor using an NAA layer. Reproduced with permission.[43a] Copyright 2007, American Chemical Society.

form the matrix of NT walls. QD gradient within the NTs was formed by layer-by-layer deposition using mercaptoundecanoic acid coated ZnCdSe alloy QDs (negatively charged). Details about the design of the structure and the method are detailed in the schematic in **Figure 9**. High sensitive detection of DNA hybridization was achieved by the versatile design developed in this study using NTs assembled with graded-bandgap QDs using FRET which involved the transfer of energy from larger bandgaps of quantum dots to smaller bandgaps Cy 5 labels (Cy5 is a fluorescent dye of cyanine dye family) of the attached DNA. FRET was clearly observed in the PL emission spectra where an increase in Cy5 emission was observed in the spectra

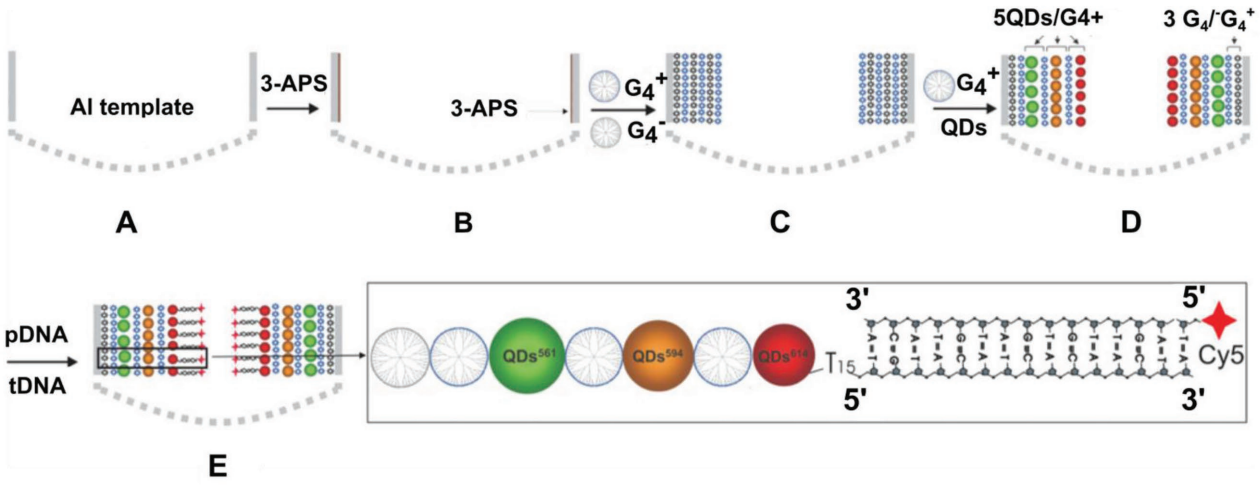

Figure 9. Schematic of nanotubes containing a graded-bandgap structure prepared by incorporating three types of ZnCdSe alloy QDs. A) Self-assembled NAA membrane is used as a template. B) The pore walls are coated with 3-aminopropyl dimethylethoxysilane (3-APS) to provide a positively charged surface. C) The first negatively charged dendrimer layer is deposited, followed by alternate deposition of positively and negatively charged dendrimers. Before the first QD layer is deposited, three bilayers of positively and negatively charged dendrimers are deposited. D) The assembly of QDs inside the template started with the deposition of QDs with luminescence maximum at k = 561 nm (QD561, green), then QDs with luminescence maximum at k = 594 nm (QD594, orange), and finally QDs with luminescence maximum at k = 614 nm (QD614, red). Five positively charged dendrimer/QD bilayers for each. E) After activation by N-hydroxysuccinimide (NHS)/1-ethyl-3(dimethylamino)propylcarbodiimide (EDC), probe DNA (pDNA) immobilization, and hybridization with Cy5-labeled complementary DNA (tDNA) can be achieved inside the NTs (see enlargement). Reproduced with permission.[81]

which is attributed to the excitation energy transfers by FRET from QDs to the Cy5. It was also found that the detection sensitivity was tunable by varying the assemblies of gradient QDs inside the NTs. This sensing strategy is very useful for detecting small but very significant changes that occur during biological detection.

5. Conclusions and Future Perspectives

NAA has been used as a versatile biosensing platform for various clinically important biomarkers. In this review, advances in NAA as a potential sensing platform for biomarker detection are examined as a result of the need for effective technology for disease detection. We have discussed the structure, properties, and their application of NAA in biosensing.

NAA prepared by anodization of high purity Al is one of the most widely used porous materials for biosensing due to its well-known advantageous properties such as simple fabrication of highly ordered nanoporous structure, large surface-to-volume ratio, tunable and well-controllable nanoporous geometry, biocompatibility, ease of functionalization, chemical stability, and also possibilities for miniaturization and mass production. NAA also exhibits excellent optical and electrochemical properties such as PL, reflectivity, transmittance, absorbance, electron transfer, impedance, electrical resistance, and conductance. These properties have been widely exploited as detection principles for developing highly sensitive biosensing platforms. Moreover, due to its highly ordered porous structure, NAA has also been used as a template in developing 3D ordered nanostructures in a highly reproducible, cost effective, and simple manner.

The use of NAA nanochannels for biosensing has led to various detection systems for biomarkers based on diverse detection strategies. These detection systems suit well for the highly sensitive analysis of biomarkers in complex body fluids such as human blood with minimal sample preparation and minimization/avoidance of matrix effects. We have discussed the relevant examples for NAA biosensors developed for the detection of biomarkers of clinical interest, including pathogens, small molecules, proteins, and nucleic acids. These sensors rely on various transduction methods, mainly electrochemical and optical. Electrochemical techniques are the most popular transduction techniques for biomarker detection using NAA material, followed by optical techniques. However, some protein sensors developed using optical techniques offer very high sensitivity and low LODs. Therefore, more research should be done to develop optical sensing platforms using NAA for biomarker detection. Most of the sensing systems reviewed here are much more sensitive and efficient than conventional detection techniques such as PCR and ELISA.

NAA-based biosensing has a potential future for the development of relevant POC devices for biomarker detection in clinical setups. NAA can be the key to obtaining highly efficient, robust, miniaturized, and portable devices for clinical applications by miniaturization and integration into lab-on-chip systems. Some studies have also demonstrated that it is possible to develop multiplex detection platforms for simultaneous detection of multiple analytes using NAA as the sensing platform. Due to the biocompatibility of NAA, it is also possible to translate this technology into implantable sensors for real time and in vivo monitoring of biomarkers.

Acknowledgements

G.R. would like to thank UniSA and Wound Management Innovation CRC for a Ph.D. scholarship. This work was also supported by the Spanish Ministry of Economy and competitiveness (MINECO), TEC2015-71324-R and by the ICREA under the 2014 ICREA Academia Award.

Conflict of Interest

The authors declare no conflict of interest.

Keywords

biomarker detection, biosensors, clinical diagnosis, nanoporous anodic alumina, porous alumina, porous materials

Received: July 29, 2017
Revised: October 6, 2017
Published online: December 5, 2017

[1] P. Sahu, N. Pinkalwar, R. D. Dubey, S. Paroha, S. Chatterjee, T. Chatterjee, *Asian J. Res. Pharm. Sci.* **2011**, *1*, 9.
[2] D. R. Thévenot, K. Toth, R. A. Durst, G. S. Wilson, *Biosens. Bioelectron.* **2001**, *16*, 121.
[3] M. Holzinger, A. Le Goff, S. Cosnier, *Front. Chem.* **2014**, *2*, 63.
[4] Z. Dai, H. Ju, *Trends Anal. Chem* **2012**, *39*, 149.
[5] A. de la Escosura-Muñiz, A. Merkoçi, *ACS Nano* **2012**, *6*, 7556.
[6] L. Vojkuvka, A. Santos, J. Pallarès, J. Ferré-Borrull, L. F. Marsal, J.-P. Celis, *Surf. Coat. Technol.* **2012**, *206*, 2115.
[7] L. F. Marsal, L. Vojkuvka, P. Formentin, J. Pallarés, J. Ferré-Borrull, *Opt. Mater.* **2009**, *31*, 860.
[8] A. Santos, T. Kumeria, D. Losic, *Trends Anal. Chem.* **2013**, *44*, 25.
[9] A. J. Atkinson, W. A. Colburn, V. G. DeGruttola, D. L. DeMets, G. J. Downing, D. F. Hoth, J. A. Oates, C. C. Peck, R. T. Schooley, B. A. Spilker, J. Woodcock, S. L. Zeger, *Clin. Pharmacol. Ther.* **2001**, *69*, 89.
[10] V. S. Vaidya, J. V. Bonventre, *Biomarkers: In Medicine, Drug Discovery, and Environmental Health*, Wiley, Hoboken, New Jersey **2010**.
[11] K. Strimbu, J. A. Tavel, *Curr. Opin. HIV AIDS* **2010**, *5*, 463.
[12] J. Hu, S. Wang, L. Wang, F. Li, B. Pingguan-Murphy, T. J. Lu, F. Xu, *Biosens. Bioelectron.* **2014**, *54*, 585.
[13] X. Xu, A. Akay, H. Wei, S. Wang, B. Pingguan-Murphy, B.-E. Erlandsson, X. Li, W. Lee, J. Hu, L. Wang, *Proc. IEEE* **2015**, *103*, 236.
[14] L. Bissonnette, M. G. Bergeron, *Clin. Microbiol. Infect.* **2010**, *16*, 1044.
[15] M. Mascini, S. Tombelli, *Biomarkers* **2008**, *13*, 637.
[16] F. Properzi, M. Logozzi, S. Fais, *Biomarkers Med.* **2013**, *7*, 769.
[17] F. Wei, J. Yang, D. T. Wong, *Biosens. Bioelectron.* **2013**, *44*, 115.
[18] L. Stoner, A. A. Lucero, B. R. Palmer, L. M. Jones, J. M. Young, J. Faulkner, *Clin. Biochem.* **2013**, *46*, 1353.
[19] T. R. Dargaville, B. L. Farrugia, J. A. Broadbent, S. Pace, Z. Upton, N. H. Voelcker, *Biosens. Bioelectron.* **2013**, *41*, 30.
[20] H. Masuda, K. Fukuda, *Science* **1995**, *268*, 1466.

[21] a) O. Nishinaga, T. Kikuchi, S. Natsui, R. O. Suzuki, *Sci. Rep.* **2013**, *3*, 2748; b) Y. Ma, Y. Wen, J. Li, Y. Li, Z. Zhang, C. Feng, R. Sun, *Sci. Rep.* **2016**, *6*, 39165.
[22] A. P. Li, F. Müller, A. Birner, K. Nielsch, U. Gösele, *J. Appl. Phys.* **1998**, *84*, 6023.
[23] a) A. M. Md Jani, D. Losic, N. H. Voelcker, *Prog. Mater. Sci.* **2013**, *58*, 636; b) R. Furneaux, W. Rigby, A. Davidson, *Nature* **1989**, *337*, 147.
[24] K. Alam, A. Singh, S. Bodepudi, S. Pramanik, *Surf. Sci.* **2011**, *605*, 441.
[25] O. Jessensky, F. Müller, U. Gösele, *Appl. Phys. Lett.* **1998**, *72*, 1173.
[26] a) H. Masuda, K. Yada, A. Osaka, *Jpn. J. Appl. Phys.* **1998**, *37*, L1340; b) H. Masuda, F. Hasegwa, S. Ono, *J. Electrochem. Soc.* **1997**, *144*, L127.
[27] a) M. M. Rahman, E. Garcia-Caurel, A. Santos, L. F. Marsal, J. Pallarès, J. Ferré-Borrull, *Nanoscale Res. Lett.* **2012**, *7*, 474; b) A. Santos, P. Formentín, J. Pallarès, J. Ferré-Borrull, L. F. Marsal, *J. Electroanal. Chem.* **2011**, *655*, 73.
[28] J. Zhang, J. E. Kielbasa, D. L. Carroll, *Mater. Chem. Phys.* **2010**, *122*, 295.
[29] A. Santos, L. Vojkuvka, J. Pallarés, J. Ferré-Borrull, L. F. Marsal, *J. Electroanal. Chem.* **2009**, *632*, 139.
[30] W. Lee, R. Ji, U. Gösele, K. Nielsch, *Nat. Mater.* **2006**, *5*, 741.
[31] S. Tanvir, J. Pantigny, P. Boulnois, S. Pulvin, *J. Membr. Sci.* **2009**, *329*, 85.
[32] A. de la Escosura-Muñiz, A. Merkoçi, *Electrochem. Commun.* **2010**, *12*, 859.
[33] D.-K. Kim, K. Kerman, S. Yamamura, Y.-S. Kwon, Y. Takamura, E. Tamiya, *Jpn. J. Appl. Phys.* **2008**, *47*, 1351.
[34] F. S. H. Krismastuti, H. Bayat, N. H. Voelcker, H. Schönherr, *Anal. Chem.* **2015**, *87*, 3856.
[35] D. Losic, M. A. Cole, B. Dollmann, K. Vasilev, H. J. Griesser, *Nanotechnology* **2008**, *19*, 245704.
[36] Y. Du, W. Cai, C. Mo, J. Chen, L. Zhang, X. Zhu, *Appl. Phys. Lett.* **1999**, *74*, 2951.
[37] G. D. Sulka, *Nanostruct. Mater. Electrochem.* **2008**, *1*, 1.
[38] A. Santos, M. Alba, M. M. Rahman, P. Formentín, J. Ferré-Borrull, J. Pallarès, L. F. Marsal, *Nanoscale Res. Lett.* **2012**, *7*, 228.
[39] A. Santos, V. S. Balderrama, M. Alba, P. Formentín, J. Ferré-Borrull, J. Pallarès, L. F. Marsal, *Adv. Mater.* **2012**, *24*, 1050.
[40] a) A. Santos, G. Macías, J. Ferré-Borrull, J. Pallarès, L. F. Marsal, *ACS Appl. Mater. Interfaces* **2012**, *4*, 3584; b) R. Jia, Y. Shen, H. Luo, X. Chen, Z. Hu, D. Xue, *Solid State Commun.* **2004**, *130*, 367.
[41] a) S. D. Alvarez, C.-P. Li, C. E. Chiang, I. K. Schuller, M. J. Sailor, *ACS Nano* **2009**, *3*, 3301; b) A. Santos, V. S. Balderrama, M. Alba, P. Formentín, J. Ferré-Borrull, J. Pallarès, L. F. Marsal, *Nanoscale Res. Lett.* **2012**, *7*, 370; c) G. Macias, L. P. Hernández-Eguía, J. Ferré-Borrull, J. Pallares, L. F. Marsal, *ACS Appl. Mater. Interfaces* **2013**, *5*, 8093.
[42] A. Santos, T. Kumeria, D. Losic, *Anal. Chem.* **2013**, *85*, 7904.
[43] a) D.-K. Kim, K. Kerman, M. Saito, R. R. Sathuluri, T. Endo, S. Yamamura, Y.-S. Kwon, E. Tamiya, *Anal. Chem.* **2007**, *79*, 1855; b) H. M. Hiep, H. Yoshikawa, E. Tamiya, *Anal. Chem.* **2010**, *82*, 1221; c) S.-H. Yeom, O.-G. Kim, B.-H. Kang, K.-J. Kim, H. Yuan, D.-H. Kwon, H.-R. Kim, S.-W. Kang, *Opt. Express* **2011**, *19*, 22882.
[44] H. Ko, V. V. Tsukruk, *Small* **2008**, *4*, 1980.
[45] Z. Lu, W. Ruan, J. Yang, W. Xu, C. Zhao, B. Zhao, *J. Raman Spectrosc.* **2009**, *40*, 112.
[46] N. Ji, W. Ruan, C. Wang, Z. Lu, B. Zhao, *Langmuir* **2009**, *25*, 11869.
[47] a) S. J. Lee, Z. Guan, H. Xu, M. Moskovits, *J. Phys. Chem. C* **2007**, *111*, 17985; b) L. Velleman, J.-L. Bruneel, F. Guillaume, D. Losic, J. G. Shapter, *Phys. Chem. Chem. Phys.* **2011**, *13*, 19587.
[48] O. Lazcka, F. J. D. Campo, F. X. Muñoz, *Biosens. Bioelectron.* **2007**, *22*, 1205.
[49] B. T. Nguyen, G. Koh, H. S. Lim, A. J. Chua, M. M. Ng, C.-S. Toh, *Anal. Chem.* **2009**, *81*, 7226.
[50] a) K. Y. Chan, W. W. Ye, Y. Zhang, L. D. Xiao, P. H. Leung, Y. Li, M. Yang, *Biosens. Bioelectron.* **2013**, *41*, 532; b) M. S. Cheng, S. H. Lau, V. T. Chow, C.-S. Toh, *Environ. Sci. Technol.* **2011**, *45*, 6453; c) F. Tan, P. H. Leung, Z.-b. Liu, Y. Zhang, L. Xiao, W. Ye, X. Zhang, L. Yi, M. Yang, *Sens. Actuators, B* **2011**, *159*, 328.
[51] a) M. S. Cheng, J. S. Ho, C. H. Tan, J. P. S. Wong, L. C. Ng, C.-S. Toh, *Anal. Chim. Acta* **2012**, *725*, 74; b) J. Deng, C.-S. Toh, *Sensors* **2013**, *13*, 7774; c) B. T. T. Nguyen, A. E. K. Peh, C. Y. L. Chee, K. Fink, V. T. Chow, M. M. Ng, C.-S. Toh, *Bioelectrochemistry* **2012**, *88*, 15; d) A. E. K. Peh, S. F. Y. Li, *Biosens. Bioelectron.* **2013**, *42*, 391; e) V. Rai, H. C. Hapuarachchi, L. C. Ng, S. H. Soh, Y. S. Leo, C.-S. Toh, *PloS One* **2012**, *7*, e42346.
[52] V. Rai, J. Deng, C.-S. Toh, *Talanta* **2012**, *98*, 112.
[53] G. Koh, S. Agarwal, P.-S. Cheow, C.-S. Toh, *Electrochim. Acta* **2007**, *52*, 2815.
[54] G. Koh, S. Agarwal, P.-S. Cheow, C.-S. Toh, *Electrochim. Acta* **2007**, *53*, 803.
[55] D. V. John, Y.-S. Lin, G. C. Perng, *J. Biomed. Sci.* **2015**, *22*, 83.
[56] C.-K. Joung, H.-N. Kim, M.-C. Lim, T.-J. Jeon, H.-Y. Kim, Y.-R. Kim, *Biosens. Bioelectron.* **2013**, *44*, 210.
[57] F. Tian, J. Lyu, J. Shi, F. Tan, M. Yang, *Sens. Actuators, B* **2016**, *225*, 312.
[58] http://www.nature.com/subjects/small-molecules, (accessed: February 2017).
[59] a) S.-J. Li, Y. Xing, M.-Y. Tang, L.-H. Wang, L. Liu, *Anal. Methods* **2013**, *5*, 7022; b) S. Maghsoodi, Z. Gholami, H. Chourchian, Y. Mortazavi, A. A. Khodadadi, *Sens. Actuators, B* **2009**, *141*, 526; c) Y. Xian, Y. Hu, F. Liu, Y. Xian, L. Feng, L. Jin, *Biosens. Bioelectron.* **2007**, *22*, 2827; d) C. Boss, E. Meurville, J.-M. Sallese, P. Ryser, presented at *Proc. Eurosensors XXIII Conf.*, Lausanne, Switzerland **2009**.
[60] a) Y. Li, H. Bai, Q. Liu, J. Bao, M. Han, Z. Dai, *Biosens. Bioelectron.* **2010**, *25*, 2356; b) E. Stura, D. Bruzzese, F. Valerio, V. Grasso, P. Perlo, C. Nicolini, *Biosens. Bioelectron.* **2007**, *23*, 655.
[61] a) Z. Yang, S. Si, C. Zhang, *Microporous Mesoporous Mater.* **2008**, *111*, 359; b) Z. Yang, C. Zhang, *Sens. Actuators, B* **2013**, *188*, 313.
[62] A. Dhathathreyan, *J. Phys. Chem. B* **2011**, *115*, 6678.
[63] a) K. Kant, J. Yu, C. Priest, J. G. Shapter, D. Losic, *Analyst* **2014**, *139*, 1134; b) K. Kant, C. Priest, J. G. Shapter, D. Losic, *Electrochim. Acta* **2014**, *139*, 225.
[64] A. Kisner, R. Stockmann, M. Jansen, U. Yegin, A. Offenhäusser, L. T. Kubota, Y. Mourzina, *Biosens. Bioelectron.* **2012**, *31*, 157.
[65] A. Wisitsoraat, C. Karuwan, K. Wong-ek, D. Phokharatkul, P. Sritongkham, A. Tuantranont, *Sensors* **2009**, *9*, 8658.
[66] M. Yuqing, G. Jianguo, C. Jianrong, *Biotechnol. Adv.* **2003**, *21*, 527.
[67] C. Boss, E. Meurville, J.-M. Sallese, P. Ryser, *Biosens. Bioelectron.* **2011**, *30*, 223.
[68] Z. Yang, S. Si, C. Zhang, *Biochem. Biophys. Res. Commun.* **2008**, *367*, 169.
[69] a) A. de la Escosura-Muñiz, A. Merkoçi, *Small* **2011**, *7*, 675; b) A. de la Escosura-Muñiz, W. Chunglok, W. Surareungchai, A. Merkoçi, *Biosens. Bioelectron.* **2013**, *40*, 24.
[70] M. Espinoza-Castañeda, A. de la Escosura-Muñiz, A. Chamorro, C. de Torres, A. Merkoçi, *Biosens. Bioelectron.* **2015**, *67*, 107.
[71] W. Ye, J. Guo, S. Chen, M. Yang, *J. Mater. Chem. B* **2013**, *1*, 6544.
[72] J. C. Lee, J. Y. An, B. W. Kim, *J. Chem. Technol. Biotechnol.* **2007**, *82*, 1045.
[73] A. C. Whelen, D. H. Persing, *Annu. Rev. Microbiol.* **1996**, *50*, 349.
[74] I. Vlassiouk, P. Takmakov, S. Smirnov, *Langmuir* **2005**, *21*, 4776.
[75] A. de la Escosura-Muñiz, A. Mekoçi, *Chem. Commun.* **2010**, *46*, 9007.

[76] S.-J. Li, J. Li, K. Wang, C. Wang, J.-J. Xu, H.-Y. Chen, X.-H. Xia, Q. Huo, *ACS Nano* **2010**, *4*, 6417.
[77] H.-L. Gao, M. Wang, Z.-Q. Wu, C. Wang, K. Wang, X.-H. Xia, *Anal. Chem.* **2015**, *87*, 3936.
[78] W. W. Ye, J. Y. Shi, C. Y. Chan, Y. Zhang, M. Yang, *Sens. Actuators, B* **2014**, *193*, 877.
[79] S. Wu, W. Ye, M. Yang, M. Taghipoor, R. Meissner, J. Brugger, P. Renaud, *Sens. Actuators, B* **2015**, *216*, 105.
[80] S. Pan, L. J. Rothberg, *Nano Lett.* **2003**, *3*, 811.
[81] C. L. Feng, X. Zhong, M. Steinhart, A. M. Caminade, J. P. Majoral, W. Knoll, *Adv. Mater.* **2007**, *19*, 1933.